Predicting of tall building response to non-stationary winds using multiple wind speed samples

Guoqing Huang[*1], Xinzhong Chen[2], Haili Liao[1] and Mingshui Li[1]

[1]*Research Center for Wind Engineering, School of Civil Engineering,*
Southwest Jiaotong University, Chengdu, Sichuan 610031, China
[2]*Wind Science and Engineering Research Center, Department of Civil and Environmental Engineering,*
Texas Tech University, Lubbock, Texas 79409, USA

Abstract. Non-stationary extreme winds such as thunderstorm downbursts are responsible for many structural damages. This research presents a time domain approach for estimating along-wind load effects on tall buildings using multiple wind speed time history samples, which are simulated from evolutionary power spectra density (EPSD) functions of non-stationary wind fluctuations using the method developed by the authors' earlier research. The influence of transient wind loads on various responses including time-varying mean, root-mean-square value and peak factor is also studied. Furthermore, a simplified model is proposed to describe the non-stationary wind fluctuation as a uniformly modulated process with a modulation function following the time-varying mean. Finally, the probabilistic extreme response and peak factor are quantified based on the up-crossing theory of non-stationary process. As compared to the time domain response analysis using limited samples of wind record, usually one sample, the analysis using multiple samples presented in this study will provide more statistical information of responses. The time domain simulation also facilitates consideration of nonlinearities of structural and wind load characteristics over previous frequency domain analysis.

Keywords: : non-stationary winds; evolutionary power spectra density function; time history samples; tall building response; extreme value distribution

1. Introduction

Non-stationary extreme winds including hurricanes or typhoons and thunderstorms are responsible for damages of many buildings and other structures in the U.S. and around the world (e.g., Twisdale and Vickery 1992, Holmes 1999, Letchford *et al.* 2001, Choi 2004). Characterizing and modeling these extreme winds have drawn more attention from meteorological and wind engineering communities (e.g., Xu and Chen 2004, Chen and Letchford 2007).   Based on full-scale observations, Fujita (1985 and 1990) characterized downburst winds with different mean wind speed vertical profiles, rapid time-varying mean wind speeds, and spatially strongly correlated wind fluctuations. The physical simulation of non-stationary winds has been conducted by Letchford and Chay (2002), Sengupta and Sarkar (2008) and others. Although it is difficult to

---

capture the downbursts in the field due to small temporal and spatial scales, and random occurrences, limited full-scale measurements were obtained by Gast and Schroeder (2003) and Choi (2004). More information about characterization and modeling, and numerical simulation of these non-stationary downbursts can be found in literature (e.g., Holmes and Oliver 2000, Wood *et al.* 2001, Chay *et al.* 2006, Kim and Hangan 2007, Mason *et al.* 2009, Li *et al.* 2012).

These non-stationary extreme winds after removing time-varying mean values can be modeled as non-stationary random processes which are often characterized in terms of time-varying spectra. The evolutionary power spectra density (EPSD) functions (e.g., Priestley 1981) prevail in engineering practice, especially for applications in stochastic structural dynamics, in that the EPSD functions have similar physical significance for non-stationary processes as the traditional power spectral density (PSD) functions for the stationary processes. The adequate estimation of the EPSD functions will be essential for characterization, modeling and simulation of these processes and their effects on structures.

With better time-frequency resolution over other tools such as the Wigner-Ville method and short-time Fourier Transform, wavelets have been adopted to develop new approach to estimate the EPSDs of non-stationary processes for both scalar case (Spanos and Failla 2004) and vector case (Huang and Chen 2009). Huang and Chen (2009) also applied this approach to estimate the EPSD of full-scale downburst winds (Gast and Schroeder 2003), and analyzed their non-stationary characteristics.

Compared to considerable research efforts on wind effects on structures under stationary boundary layer winds, the understanding of non-stationary extreme wind effects such as thunderstorm downbursts has been less developed. Chen and Letchford (2004a) studied building responses in the time domain using a single sample of downburst wind. Holmes *et al*. (2005) computed the dynamic response spectrum of single-degree-of-freedom (SDOF) structures excited by a thunderstorm wind, which is similar to the response spectrum widely used in earthquake engineering. Recently, Chen (2008) developed a frequency domain framework for quantifying tall building response caused by non-stationary winds using the evolutionary power spectra. Within this framework, the influence of the time-varying mean wind speed, mean wind speed vertical profile, spatial correlation of wind fluctuations on building dynamic response was addressed.

Kwon and Kareem (2009) presented a general gust-front factor framework for modeling transient wind load effects on structures. Simulation of non-stationary winds based on the estimated EPSD offers a new opportunity to evaluate the non-stationary wind effects on buildings and improve the understanding of the interaction between the non-stationary wind and the structure. It is noted that the simulation of non-stationary winds could also been obtained through other approaches, such as the time-varying autoregressive model (e.g., Chen 2005, Chen and Letchford 2007).

In this paper, a time domain analysis framework is employed for estimating tall building responses to non-stationary winds. This framework involves estimation of the EPSD of non-stationary wind speed based on the method proposed by Huang and Chen (2009), simulation of non-stationary wind time history using the spectral representation method (e.g., Deodatis 1996a, b), calculation of time history of wind load, and determination of response history by using the step-by-step integration method. From multiple response time histories, the time-dependent statistics such as RMS and extreme value of response are determined. The results are compared with those obtained from the frequency domain analysis (Chen 2008). Furthermore, a simplified model of non-stationary wind fluctuation is proposed, and the resulting building response is addressed. The influence of transient non-stationary winds on the extreme value of building

response, gust response factor (GRF) and peak factor is also studied. Finally, the probabilistic extreme and peak factor of building response are quantified based on the up-crossing theory of non-stationary response processes.

As compared to the time domain response analysis using single sample of wind record (e.g., Holmes *et al*. 2005), the analysis using multiple samples presented in this study will provide the statistical information of responses, such as time-varying RMS value of the response and extreme value. The time domain simulation also facilitates consideration of nonlinearities of structural and wind load characteristics not accounted in the frequency domain analysis (Chen 2008).

2. Time domain response analysis framework

The following time domain response analysis framework is developed largely based on the approach presented by Chen (2008). Consider the along-wind response of a tall building under the action of a non-stationary wind. The wind speed at elevation z above the ground, $U(z,t)$, can be decomposed into the time-varying mean and fluctuating component as

$$U(z,t) = \bar{U}(z,t) + u'(z,t) \tag{1}$$

The fluctuating component $u'(z,t)$ is modeled as a zero mean evolutionary random process and can be generally expressed as follows

$$u'(z,t) = \int_{-\infty}^{\infty} e^{i\omega t} d\Theta(z,\omega,t) \tag{2}$$

where $i = \sqrt{-1}$; ω is circular frequency; $d\Theta(z,\omega,t)$ is complex-valued zero-mean orthogonal increment random process with the following properties

$$E[d\Theta(z,\omega,t)] = 0 \tag{3}$$

$$d\Theta(z,\omega,t) = d\Theta^*(z,-\omega,t) \tag{4}$$

$$E[d\Theta(z_1,\omega_1,t)d\Theta^*(z_2,\omega_2,t+\tau)] = S_u(z_1,z_2,\omega_1,t)e^{i\omega\tau}\delta(z_1-z_2)\delta(\omega_1-\omega_2)d\omega_1 d\omega_2 \tag{5}$$

where $E[\ldots]$ is expectation or ensemble average; $*$ denotes the complex conjugation; $\delta(\ldots)$ is Dirac delta function; τ is time lag; $S_u(z_1,z_2,\omega_1,t)$ is the cross EPSD between $u'(z_1,t)$ and $u'(z_2,t)$; and $S_u(z,\omega,t) = S_u(z,z,\omega,t)$ is EPSD of $u'(z,t)$.

Following the strip theory (e.g., Holmes 2001), the along-wind force per unit height of the building at the elevation z is quantified as the summation of the time-varying mean component, $\bar{P}(z,t)$, and fluctuating component, $P'(z,t)$

$$\bar{P}(z,t) = 0.5\rho C_D B \bar{U}^2(z,t) \tag{6}$$

$$P'(z,t) = \rho C_D B \bar{U}(z,t) \int_{-\infty}^{\infty} \chi_D(\omega)e^{i\omega t} d\Theta(z,\omega,t) \tag{7}$$

where ρ is the air density; B is the building width; C_D is the drag coefficient; $\chi_D(\omega)$ is the complex-valued aerodynamic admittance function representing the transfer function between approaching wind fluctuation and wind force. Strictly, the aerodynamic admittance function is also a function of time for non-stationary winds.

For tall buildings, the wind-induced response is usually dominated by the fundamental modal response, and higher mode contributions can be neglected. The time-varying mean component and fluctuating component of the generalized force, $Q(t)$, in the fundamental mode are computed by

$$\bar{Q}(t) = \int_0^H \bar{P}(z,t)\Phi(z)dz \tag{8}$$

$$Q'(t) = \int_0^H P'(z,t)\Phi(z)dz \tag{9}$$

where $\Phi(z) = (z/H)^\beta$ is the fundamental modal shape; H is the building height; and β is the mode shape exponent varying from 1.0 to 1.5.

The EPSD of the $Q'(t)$ can be given as (Chen 2008)

$$S_{Q'}(\omega,t) = \int_0^H \int_0^H (\rho C_D B)^2 \bar{U}(z_1,t)\bar{U}(z_2,t)\left(\frac{z_1}{H}\right)^\beta \left(\frac{z_2}{H}\right)^\beta |\chi_D(\omega)|^2 S_u(z_1,z_2,\omega,t)dz_1dz_2 \tag{10}$$

The time-varying mean speed is assumed to be modeled as

$$\bar{U}(z,t) = \bar{U}_0(z)d(t) \tag{11}$$

where $\bar{U}_0(z)$ is the time-invariant vertical profile; and $d(t)$ is the modulation function of the mean wind speed. The vertical profile can be normalized as

$$\tilde{U}(z) = \bar{U}_0(z)/U_{max} \tag{12}$$

where U_{max} is the maximum wind speed on $\bar{U}_0(z)$. Three empirical vertical profile models for thunderstorm downburst can be found in Oseguera and Bowles (1998), Vicroy (1992) and Wood *et al.* (2001). In this study, normalized Wood's model will be employed, which is given by

$$\tilde{U}(z) = 1.55\left(\frac{z}{\delta}\right)^{1/6}\left[1 - \text{erf}(0.7\frac{z}{\delta})\right] \tag{13}$$

where δ is the height where the velocity reaches half its maximum value and $\text{erf}(x) = 2/\sqrt{\pi}\int_0^z e^{-x^2}dx$ denotes the error function. For the time function $d(t)$, typical empirical models have been proposed by Holmes and Oliver (2000) and Chay *et al.* (2006).

Accordingly, the mean generalized force is given by

$$\bar{Q}(t) = \bar{A}Q_R d^2(t) \tag{14}$$

where $\bar{A} = [\int_0^H \tilde{U}^2(z)(z/H)^\beta dz]/H$, and $Q_R = 0.5\rho C_D BHU_{max}^2$.

The EPSD of wind fluctuation, $u'(z,t)$, is assumed to be identical at all heights of the building, i.e.

$$S_{u'}(z,\omega,t) = S_{u'}(\omega,t) \tag{15}$$

The coherence function between $u'(z_1,t)$ and $u'(z_2,t)$ is assumed to be time-independent, and given as

$$\text{Coh}(z_1,z_2,\omega) = S_{u'}(z_1,z_2,\omega,t)/S_{u'}(\omega,t) = \exp\left(-\frac{k_z\omega|z_1-z_2|}{2\pi U_{max}}\right) \tag{16}$$

where k_z is the decay factor.

The EPSD of the generalized force given by Eq. (10) can be reduced to the following expression

$$S_{Q'}(\omega,t) = 4Q_R^2 S_{u'}(\omega,t)d^2(t)|\chi_D(\omega)|^2 |J_z(\omega)|^2 / U_{max}^2 \tag{17}$$

where the joint acceptance function $|J_z(\omega)|^2$ is given as

$$|J_z(\omega)|^2 = \frac{1}{H^2}\int_0^H\int_0^H \tilde{U}(z_1)\tilde{U}(z_2)\left(\frac{z_1}{H}\right)^\beta \left(\frac{z_2}{H}\right)^\beta \text{Coh}(z_1,z_2,\omega)dz_1dz_2 \tag{18}$$

For the purpose of simulating the time histories of the generalized force, the EPSD of the generalized force is further approximated as

$$S_{Q'}(\omega,t) = 4Q_R^2 S_{u'}(\omega,t)d^2(t)|\chi_D(\omega_1)|^2 |J_z(\omega_1)|^2 / U_{max}^2 \tag{19}$$

where $\omega_1 = 2\pi f_1$ is the fundamental natural frequency of the building.

As compared to Eq. (17), although this approximation results in a different EPSD of the generalized force at other frequencies it leads to almost the same building response because the resonant component dominates the total dynamic response and the building response can be regarded as the narrow band process around the building natural frequency. According to Eq. (19) and assuming the variation rate of $d(t)$ is relatively slow compared to the structural natural frequencies, the time history of the generalized force $Q'(t)$ can be directly related to a non-stationary wind fluctuation $u_0'(t)$ by

$$Q'(t) = 2Q_R u_0'(t)d(t)|\chi_D(\omega_1)||J_z(\omega_1)|/U_{max} \tag{20}$$

where $u_0'(t)$ is characterized by its EPSD $S_{u'}(\omega,t)$.

Therefore, $Q'(t)$ can be generated by first simulating $u_0'(t)$ through its EPSD $S_{u'}(\omega,t)$. It should be mentioned that a more accurate simulation of the time histories of $Q'(t)$ can be achieved based on Eq. (17) by using the rational function approximate technique (Chen *et al.* 2000).

Based on the expressions for the mean and dynamic generalized forces, i.e., Eqs. (14) and (20), it can been seen that the effects of different mean wind speed vertical profiles on the generalized forces are reflected by the different constant coefficients $\overline{A}$ and $|J_z(\omega_1)|^2$. Hence, different profiles do not alternate the dynamic characteristics of the structural responses. This observation is consistent with the study by Chen (2008).

With the knowledge of the time histories of the generalized force, the generalized displacement, velocity and acceleration and other building response components can be determined using Newmark's step-by step integration method to solve the following equation of building motion

$$M[\ddot{q}'(t) + 2\xi\omega_1\dot{q}'(t) + \omega_1^2 q'(t)] = Q'(t) \tag{21}$$

where M, ξ, and $q'(t)$ are the fundamental generalized mass, damping ratio and displacement, respectively. In addition, the mean component of the generalized displacement can be directly computed from the quasi-static analysis as $\overline{q}(t) = \overline{Q}(t)/(M\omega_1^2)$.

The mean and dynamic components of other response, $R(t)$, i.e., $\overline{R}(t)$ and $R'(t)$, are then given as

$$\overline{R}(t) = B\overline{q}(t); \quad R'(t) = Bq'(t) \tag{22}$$

where B is the modal participation coefficient.

The building velocity and acceleration are of interest for the building habitability evaluation. Their values at elevation z are determined by the dynamic components of generalized velocity and acceleration as

$$v(z,t) = \Phi(z)\dot{q}'(t) \approx \Phi(z)\omega_1 q'(t) \tag{23}$$

$$a(z,t) = \Phi(z)\ddot{q}'(t) \approx \Phi(z)\omega_1^2 q'(t) \tag{24}$$

Based on the multiple samples of response time histories, the instantaneous RMS value, the mean extreme values of response can be determined. In the following discussion, the top displacement or its extreme value is normalized by $\overline{q}_R(t) = Q_R(t)/(M\omega_1^2)$, which is the static displacement under load Q_R. The GRF and peak factor are defined as

$$\text{GRF} = \mu_{r,\max}/R_{\text{static}}^{\max} \tag{25}$$

$$g = (\mu_{r,\max} - R_{\text{static}}^{\max})/\sigma_r^{\max} \tag{26}$$

where $\mu_{r,\max}$ is the mean of extreme value of total response including the deterministic mean and random fluctuating components calculated by ensemble average; $R_{\text{static}}^{\max}$ is the maximum static response; $\sigma_r^{\max}$ is the maximum RMS response.

3. Comparison with frequency domain analysis

A shear building with a height of $H = 200$ m and a square section of $B = D = 40$ m is studied. The fundamental modal frequency is given by the empirical formula $f_1 = 46/H$. The modal damping ratio is $\xi = 1\%$, and fundamental modal shape is assumed to be linear, i.e., $\beta = 1.0$. The aerodynamic admittance function is given by Davenport's formula as

$$\left|\chi_D(\omega)\right|^2 = 2/\lambda_y(1-1/\lambda_y+1/\lambda_y e^{-\lambda_y}) \tag{27}$$

where $\lambda_y = k_y fD/U_{max}$; k_y is decay factor and taken as 8. In Wood's profile, H/δ is taken as 0.75. The decay factor for the coherence of wind fluctuations at different heights is $k_z = 8$. These parameters and models will also be used in following sections.
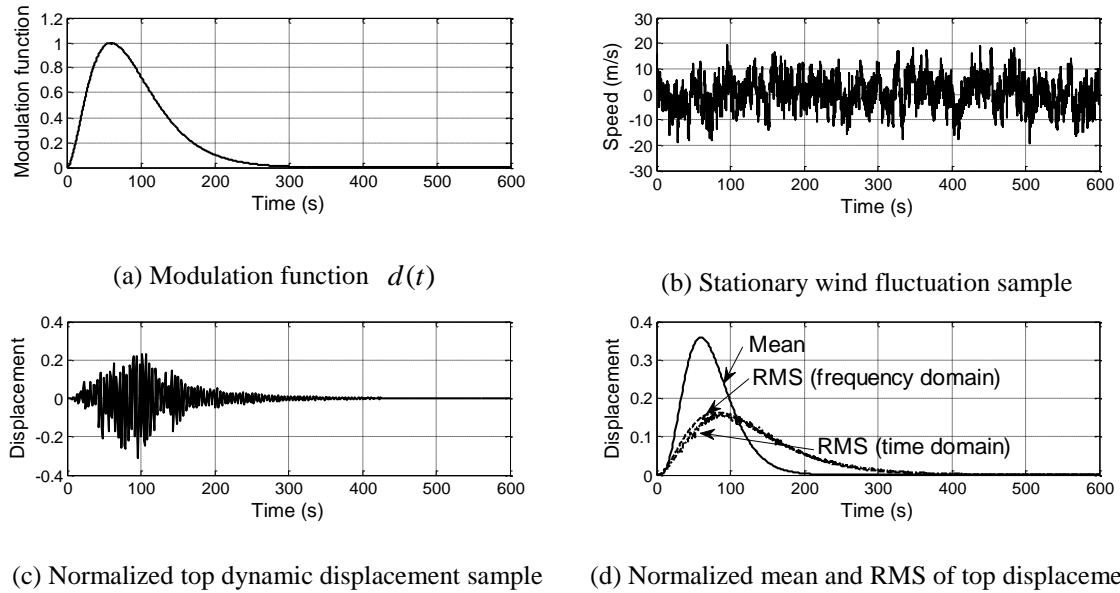

(a) Modulation function $d(t)$

(b) Stationary wind fluctuation sample

(c) Normalized top dynamic displacement sample

(d) Normalized mean and RMS of top displacement

Fig. 1 Comparison with frequency domain approach ($H = 200$ m, $U_{max} = 40$ m/s)

The numerical example used by Chen (2008) for frequency domain analysis is reevaluated by the time domain approach presented here. The modulation function of the mean wind speed, $d(t)$, with a maximum amplitude at 60 s is shown in Fig. 1(a). The maximum mean wind speed on the profile is $U_{max} = 40$m/s. The wind fluctuation of this wind event is modeled as a uniformly modulated process from a stationary wind fluctuation, i.e., with the modulation function $d(t)$. Similar treatment has adopted by Chen and Letchford (2004b) in response analysis, where the effects of the wind characteristics such as the coherence were studied. The stationary wind fluctuation is modeled by the von Karman spectrum with an integral length scale of 80 m and turbulence intensity of 15%.

The spectral representation method is applied to generate both stationary and non-stationary wind fluctuation samples (e.g., Deodatis 1996a, b). The method is based on the spectral representation theorem, which states that a process can be assigned with an orthogonal increment

process. The major procedure to derive the sample can be summarized as: at specified time instant, the spectral matrix can be discretized on a series of frequencies; then the spectral matrix can be decomposed to generate the uncorrelated components; finally, the sample can be obtained from the summation of the trigonometric items with spectral contents as coefficients. For the stationary case, the fast Fourier transform can be used to dramatically enhance the simulation efficiency. More detailed discussions can be found in (Deodatis 1996a, b).

A total of 100 time history samples were generated. The upper cutoff frequency is 10 Hz, and frequency increment is 0.00122 Hz. The generated time history samples have the time resolution of 0.05 s and time period of 819.2 s. Fig. 1(b) shows one sample of the stationary wind fluctuation. The corresponding building top dynamic displacement calculated using Newmark's method is shown in Fig. 1(c). Based on multiple samples of the response time histories, the instantaneous RMS can be computed. The normalized static and time-varying RMS values of the building top displacement are compared in Fig. 1(d).

The results show that both approaches offer almost the same results for the time-varying RMS value of response. This comparison also demonstrates the adequacy of the approximation in the generation of the time histories of the generalized force for the response prediction, i.e., Eq. (20). The GRF and peak factor are calculated as 1.71 and 1.84, respectively.

4. Response to non-stationary winds generated by evolutionary spectra

4.1 Characteristics of transient building response

In this case study, a full-scale measurement of a rear-flank downburst wind speed at height 15 m was used (Gast and Schroeder 2003). The time-varying mean and fluctuation components were derived using the discrete wavelet transform as described in Huang and Chen (2009), where the wavelet was chosen as Daubechies wavelet (e.g., Daubechies 1992) of order 3 with decomposition level 5. Level 5 is equivalent to a window size of 32 s for the time-varying mean component with a frequency range below 0.016 Hz. The maximum time-varying mean wind speed is 32.15 m/s.

Fig. 2 shows the modulation function of the mean wind speed, $d(t)$, which is defined as the time-varying mean wind speed divided by the maximum wind speed. Based on the framework for estimating EPSD proposed by Huang and Chen (2009), the normalized EPSD of the wind fluctuation is shown in Fig. 3, where length scale is $L_u = 168$ m. This length scale was derived from the corresponding stationary fluctuation of the original non-stationary wind speed, as shown in next section.
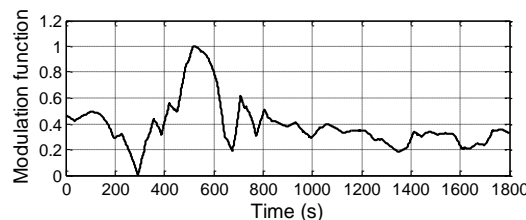

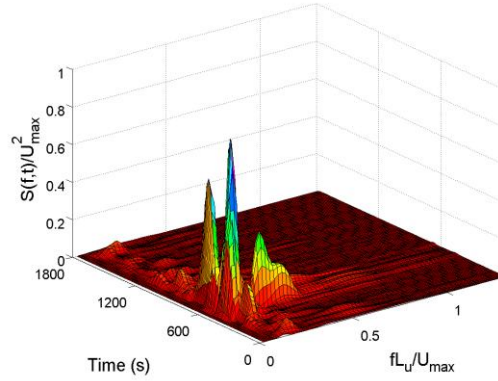Fig. 2 Modulation function from field observation record of non-stationary wind

Fig. 3 Normalized EPSD of the non-stationary wind fluctuation

Based on the modulation function of the mean wind speed and the estimated EPSD, non-stationary wind time histories with a given maximum wind speed were generated using the spectral representation method (e.g., Deodatis 1996b). A total of 100 time history samples of the wind fluctuation were generated. The corresponding building responses were then calculated.

From each sample of simulated response, the extreme value of the response was quantified. Then the mean and RMS of the extreme values were calculated. In addition, responses of buildings with heights $H = 100, 150, 250$ and 300 m with $B = D = 40$ m were also investigated. Fig. 4 shows the mean and RMS of extreme values of top displacements of the buildings. The building response at $U_{max} = 32.15$ m/s directly using the original single wind speed record is also calculated for comparison. As shown in Fig. 4, the results computed from the original sample lies within those obtained from the simulated samples. The acceptable difference between the response from the original sample and those averaged from the multiple simulated samples is attributed to the difference in the spectral values around the natural frequency.
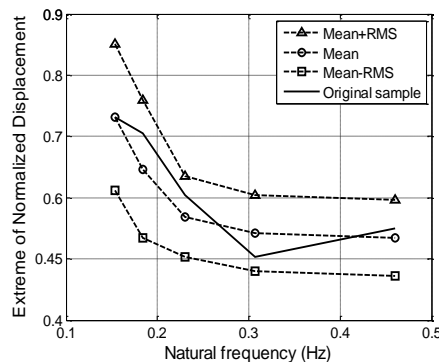
Fig. 4 Comparison of estimated building top displacement using original one sample and simulated multiple samples of wind fluctuations ($U_{max} = 32.15$ m/s)
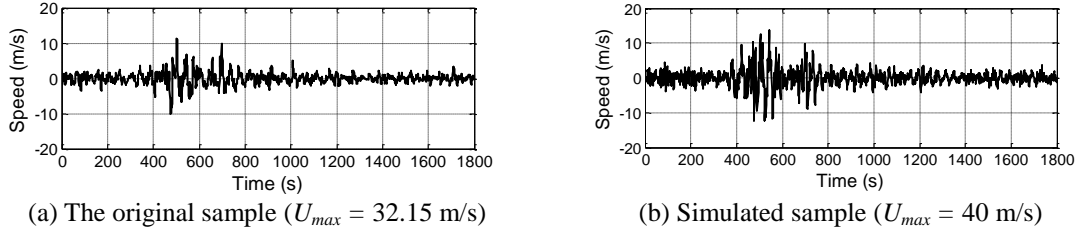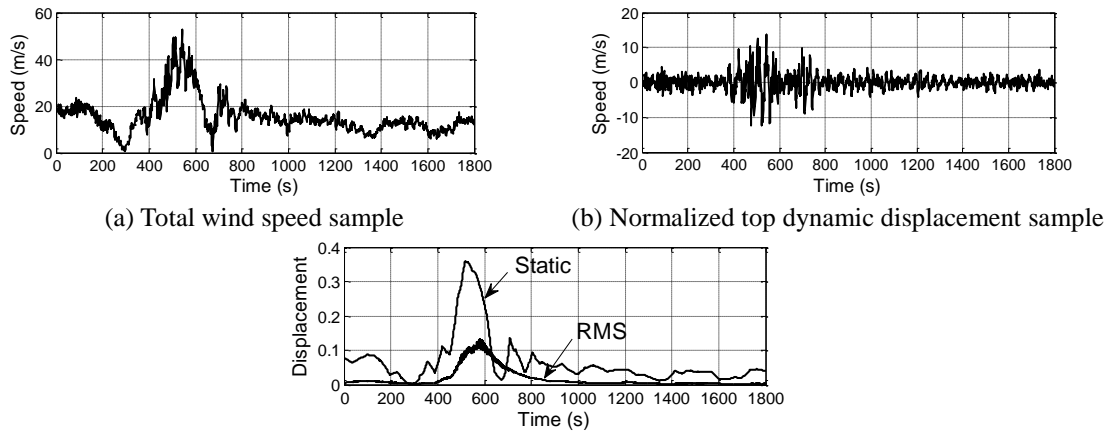
(a) The original sample (U_{max} = 32.15 m/s)

(b) Simulated sample (U_{max} = 40 m/s)

Fig. 5 Two samples of nonstatioanry wind fluctuation

(a) Total wind speed sample

(b) Normalized top dynamic displacement sample

(c) Normalized static and RMS values of top displacement

Fig. 6 Wind speed and building top displacement (H = 200 m , U_{max} = 40 m/s)

Table 1 Comparison of different wind events (H =200 m, $U_{max} = 40$ m/s)

		Case 1	Case 2	Case 3	Case 4
Maximum RMS		0.126	0.148	0.125	0.146
Mean extreme	Time domain	0.59	0.69	0.58	0.85
	Upcrossing	0.59	0.72	0.6	0.86
GRF	Time domain	1.64	1.92	1.61	2.36
	Upcrossing	1.64	2	1.67	2.39
Peak factor	Time domain	1.83	2.23	1.76	3.36
	Upcrossing	1.83	2.43	1.92	3.42

Note: Case 1: time-varying mean   [$d(t) \leq 1$]+ non-stationary fluctuation [$u_0'(t)$];

Case 2: time-invariant mean [$d(t) = 1$]+ non-stationary fluctuation [$u_0'(t)$];

Case 3: time-varying mean   [$d(t) \leq 1$]+ simplified non-stationary fluctuation [$u(t)d(t)$];

Case 4: time-invariant mean [$d(t) = 1$]+ stationary fluctuation [$u(t)$].

Fig. 5 demonstrates the original sample of the non-stationary fluctuation with U_{max} = 32.15 m/s and a simulated sample of the fluctuation with U_{max} = 40 m/s. Corresponding to Fig. 5(b), the time histories of total wind speed (including the time-varying mean and fluctuating component) and the top dynamic displacement are illustrated in Figs. 6(a) and 6(b). The static and RMS values of the normalized building top displacement are depicted in Fig. 6(c). The maximum normalized static response is 0.36. It is observed that the maximum value of the RMS response appears slightly later in time than the maximum static response. This time lag is also reported by other authors (e.g., Solomos and Spanos 1984, Conte and Peng 1997, Chen 2008). The maximum RMS, mean extreme value, GRF and peak factor are summarized in the Table 1 (Case 1).

4.2 Influence of time-varying mean wind speed

(a) Total wind speed sample [$d(t) = 1$]   (b) Normalized top dynamic displacement sample

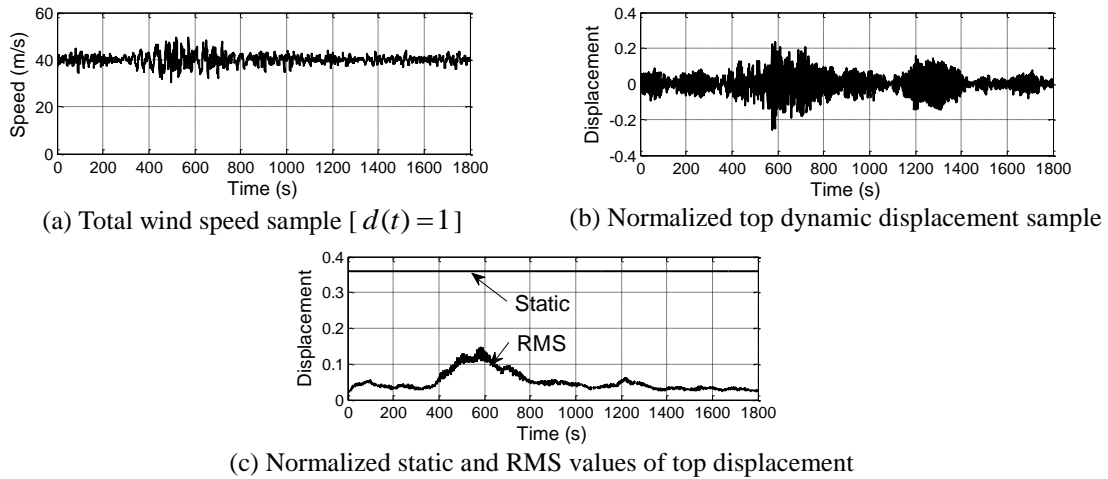(c) Normalized static and RMS values of top displacement

Fig. 7 Wind speed and building top displacement ($H = 200$ m, $U_{\max} = 40$ m/s)

To evaluate the influence of the time-varying mean on the building response, the analysis using a time-invariant mean wind speed, i.e., $d(t) = 1$, but same non-stationary wind fluctuation is also conducted. The previous case with time-varying mean wind speed and non-stationary wind fluctuation is referred to as "Case 1". The case discussed here is referred to as "Case 2". The time histories of total wind speed and building top dynamic displacement, which correspond to the wind fluctuation in Fig. 5(b), are shown in Figs. 7(a) and 7(b). The normalized static and time-varying RMS values of top displacement are shown in Fig. 7(c). The maximum RMS, mean extreme value, GRF and peak factor are summarized in the Table 1. It is seen that the maximum value of RMS response is larger than that of Case 1. The main reason is attributed to slower fluctuation variation of the generalized force in Case 2, which needs less "build-up" time. This time is the one required to take $e^{-2\xi\omega_1 t}$ close to unity (Chen 2008). Apparently, a large value of $\xi\omega_1$ requires less "build-up" time to reach the steady state response. Accordingly, the peak factor in Case 2 is also larger than that in Case 1 due to more developing time for the extreme value.

5. Simplified modeling of non-stationary wind fluctuation

In engineering practice, the non-stationary wind fluctuation may be approximately modeled as a uniformly modulated process with its modulation function following the mean wind speed, i.e., $\overline{U}_0(t) = d(t)\,U_{max}$ and $u'_0(t) = d(t)u(t)$.

The modulation function of the mean wind speed is shown in Fig. 2. The original wind fluctuation $u'_0(t)$ is shown in Fig. 5(a). Based on aforementioned approximation model, stationary wind fluctuation $u(t)$ is obtained by dividing the original fluctuation sample $u'_0(t)$ with the corresponding modulation function $d(t)$, and then by removing outliers, as shown in Figs. 8 (a) and 8(b). Note that the outliers can be removed by setting the threshold of 3-9σ_u where σ_u is the standard deviation of wind fluctuations $u(t)$. In this study, the threshold of 6σ_u is used.

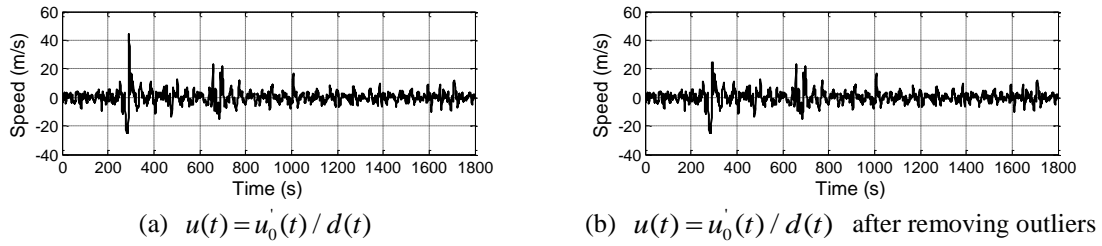(a) $u(t) = u'_0(t)\,/\,d(t)$ (b) $u(t) = u'_0(t)\,/\,d(t)$ after removing outliers

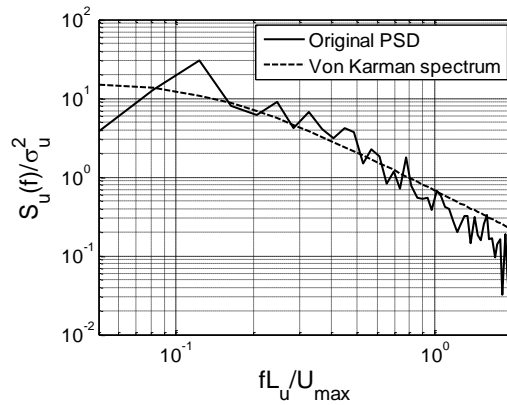Fig. 8 Derivation of the stationary fluctuation sample $u(t)$ (U_{max}=32.15 m/s)

Fig. 9 Comparison of normalized PSDs of stationary wind fluctuation

The PSD of the process $u(t)$, $S_u(f)$, is estimated and fitted with the von Karman spectrum model. The length scale and turbulence intensity are 168 m and 15%, respectively. Fig. 9 compares the PSD estimated from the sample and the one fitted by the von Karman spectrum. It can be seen

that both have a satisfactory match around the reduced frequency range of $fL_U/U_{max} = 02\text{-}1.0$, i.e., $f/U_{max} = 1.2\times10^{-3}\text{-}6.0\times10^{-3}$, which covers the fundamental frequencies of tall buildings with a certain rage of wind speed. For tall building with height of $H = 200$ m and fundamental frequency of $f = 0.23$ Hz, the corresponding wind speed range is 38 m/s-192 m/s. The fitted spectrum is used to generate 100 samples of $u(t)$ and thus $u'_0(t)$ for estimating the building response. This calculation is referred to as "Case 3".

Fig. 10 shows one sample of the stationary fluctuation $u(t)$, and the corresponding uniformly modulated fluctuation $u'_0(t) = d(t)u(t)$ with $U_{max} = 40$ m/s. Figs. 11(a) and 11(b) shows the time histories of total wind speeds and corresponding normalized building top dynamic displacement. The time-varying static and RMS values of top displacement calculated from multiple samples are shown in Fig. 11(c). The maximum RMS mean extreme, GRF and peak factor are summarized in Table 1 (Case 3).
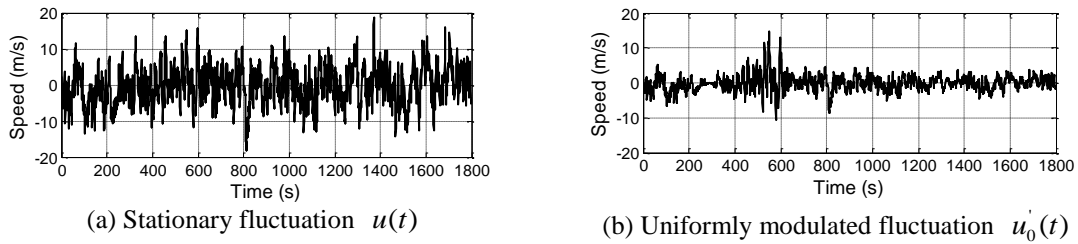

(a) Stationary fluctuation $u(t)$ (b) Uniformly modulated fluctuation $u'_0(t)$

Fig. 10 Simulated sample of wind fluctuation ($U_{max} = 40$ m/s)

(a) Total wind speed sample   (b) Normalized top dynamic displacement sample

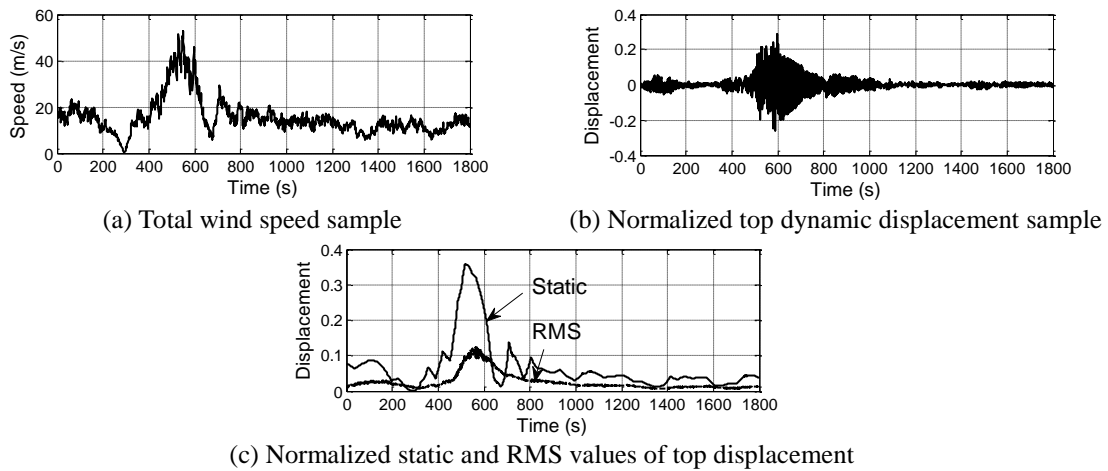(c) Normalized static and RMS values of top displacement

Fig. 11 Wind speed and building top displacement ($H = 200$ m, $U_{max} = 40$ m/s)

The comparison between Cases 1 and 3 for other wind speeds, i.e., 50 and 60 m/s, is summarized in Table 2. The results in Tables 1 and 2 show that two different approaches in

modeling the non-stationary downburst fluctuation have similar results in terms of the maximum RMS and the mean extreme value of the building response, although they offer different time histories and time-varying RMS values of response. These two approaches generate different wind fluctuations and corresponding generalized forces. However, their spectra around the building natural frequency are almost identical, which leads to almost identical building response due to the property of narrow-band filter of the mechanical transfer function of high-rise buildings. Therefore, it may be practicable to model the non-stationary fluctuation as a uniformly modulated process with the modulation function of time-varying mean speed. However, in the case of middle- and low-rise buildings, these two approaches may not lead to similar building responses due to broader frequency content of wind loads influencing the building response. In such a case, wind fluctuations generated from EPSD will offer more detailed time-frequency information of wind and wind load, and thus provide more accurate estimate of building response.

Table 2 Comparison of Cases 1 and 3 under different wind speeds (H =200 m)

	$U_{max} = 40$ m/s		$U_{max} = 50$ m/s		$U_{max} = 60$ m/s	
	Case 1	Case 3	Case 1	Case 3	Case 1	Case 3
Maximum RMS	0.126	0.125	0.142	0.140	0.144	0.148
Mean extreme	0.59	0.58	0.65	0.64	0.64	0.65
GRF	1.64	1.61	1.81	1.78	1.78	1.81
Peak factor	1.83	1.76	2.04	2.00	1.94	1.96
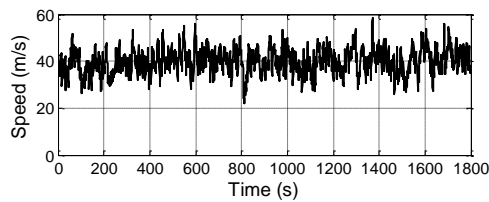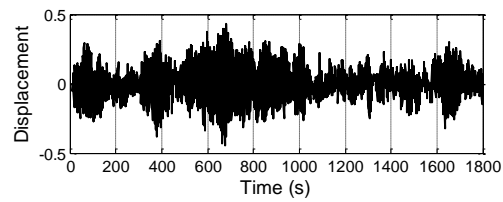
(a) Total wind speed sample [$d(t)=1$]   (b) Normalized top dynamic displacement sample

Fig. 12 Wind speed and building top displacement ($H = 200$ m, $U_{max} = 40$ m/s)

To further understand the transient wind load effect on the building response, the building response under stationary wind fluctuation $u(t)$ and mean wind speed of 40 m/s is also calculated. This is referred to as "Case 4". The time history samples of total wind speeds and building top displacement are shown in Fig. 12. The maximum RMS, GRF and peak factor of this case are summarized in Table 1. Compared to other three cases, the maximum RMS of Case 4 is almost identical, while the GRF and peak factor are much larger. The maximum RMS is mainly influenced by the wind fluctuation around the maximum mean wind speed. On the other hand, the

extreme value as reflected by GRF and peak factor depends the time-varying RMS and the time duration. Unlike Cases 1 to 3, Case 4 has a constant RMS and has a sufficient time to reach a larger extreme value. The influence of transient winds on the extreme response over a given time period can also be well understood from the upcrossing theory of non-stationary response, which is to be discussed in the next section.

6. Extreme value of non-stationary response based on upcrossing theory

The extreme value of a non-stationary Gaussian response process $R(t)$ over a given time period T can also be estimated based on upcrossing theory. Following "Poisson approximation of crossings", the mean upcrossing rate at level of r at any time t can be given by (e.g., Lutes and Sarkani 2004)

$$\nu(r,t) = \frac{\sigma_{\dot{R}}(t)}{2\pi\sigma_R(t)} \exp\left[-\frac{(r-\mu_R(t))^2}{2\sigma_R^2(t)} \right] \tag{28}$$

where $\mu_R(t)$ and $\sigma_R(t)$ are the time-varying mean and RMS of $R(t)$, respectively; and $\sigma_{\dot{R}}(t)$ is the time-varying RMS of $\dot{R}(t)$, i.e., the time derivative of $R(t)$. As the building response $R(t)$ can be regarded as a narrow band process with the central frequency of the building natural frequency ω_1, $\sigma_{\dot{R}}(t)/\sigma_R(t) \approx \omega_1$ (e.g., Lutes and Sarkani 2004).

The cumulative distribution function (CDF) of the extreme value of $R(t)$ over a time period, T, is given as (e.g., Lutes and Sarkani 2004)

$$Q_{\max}(r) = \exp[-\int_0^T \nu(r,t)dt] \approx \exp[-\exp(-\alpha_r(r-\hat{r}))] \tag{29}$$

The mode $\hat{r}$ and dispersion parameter $1/\alpha_r$ are determined by linearly fitting the curve $-\ln[-\ln(Q_{\max}(r))]$ as a function of r. The mean and RMS of the extreme value are subsequently quantified as

$$\mu_{r,\max} = \hat{r} + \frac{0.5772}{\alpha_r}, \quad \sigma_{r,\max} = \frac{\pi}{\sqrt{6}} \frac{1}{\alpha_r} \tag{30}$$

It is noted for a stationary process where $\nu(r,t) = \nu(r)$, the aforementioned formula reduces to that provided by Davenport (1964).

Fig. 13 plots the CDF of the extreme response for Cases 1 to 4. The mean extreme values, corresponding GRFs and peak factors for these 4 cases are summarized in Table 1. It is seen that the results from the up-crossing approach is very close to those from the time domain simulation. It should be noted that the coefficient of variation of extreme value $\sigma_{r,\max}/\mu_{r,\max}$ for these 4 cases varies from 10% to 13%, which is close to that of the corresponding stationary case.

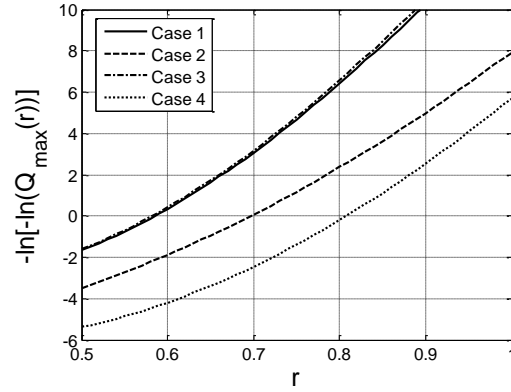Fig. 13 CDF of the extreme response

7. Conclusions

A time domain analysis framework was presented for estimating along-wind tall building response excited by non-stationary wind events. Comparison of the response analysis results with those from the frequency domain approach showed that the time domain approach offered very agreeable estimations of non-stationary response characteristics. Based on the multiple samples of wind fluctuations simulated from the estimated EPSD and the calculated building responses, the transient nature in non-stationary wind was found to lead a smaller and lagged maximum RMS value and a smaller peak response due to less "build-up" time.

A simplified model was proposed to describe the non-stationary wind fluctuation as a uniformly modulated process with a modulation function as the time-varying mean. Response analysis using this model illustrated that almost the same response characteristics were obtained. This was attributed to the fact that the along-wind response of the tall building was dominated by the wind spectra around the natural frequency, which were almost unaffected by the approximate modeling. It should be noted that in the case of middle- and low-rise buildings, the simulation using wavelets-based EPSD will offer more detailed time-frequency information of non-stationary wind fluctuations and leads to more adequate estimation of their effects on buildings.

The approach based on the mean up-crossing rate of non-stationary process provided not only the similar extreme values of the response compared to those from the time domain simulation, but more detailed information of the influence of the instantaneous statistics on the extreme value. Compared to the corresponding stationary response, the non-stationary stationary response has a smaller peak factor and GRF because the extreme response had insufficient time duration to develop.

It was noted that the effects of transient aerodynamics, i.e., instantaneous wind load characteristics such as admittance and coherence function associated with transient winds should also be considered in the future work. These effects may be remarkable when the variation rate of wind speed is large as compared to the time scale of generation of wind loads. Their characterization would require a comprehensive wind tunnel study under non-stationary wind excitations.

Acknowledgments

References

Chay, M.T., Albermani, F. and Wilson, R. (2006), "Numerical and analytical simulation of downburst wind loads", *Eng. Struct.*, **28**(2), 240-254.
Chen, L. and Letchford, C.W. (2004a), "Parametric study on the alongwind response of the CAARC building to downbursts in the time domain", *J. Wind. Eng. Ind. Aerod.*, **92**(9), 703-724.
Chen, L. and Letchford, C.W. (2004b), "A deterministic–stochastic hybrid model of downbursts and its impact on a cantilevered structure", *Eng. Struct.*, **26**, 619-629.
Chen, L. (2005), *Vector time-varying autoregressive (TVAR) models and their application to downburst wind speeds*, Ph.D. Dissertation, Texas Tech University.
Chen, L. and Letchford, C.W. (2007), "Numerical simulation of extreme winds from thunderstorm downbursts", *J. Wind. Eng. Ind. Aerod.*, **95**, 977-990
Chen, X. (2008), "Analysis of alongwind tall building response to transient nonstationary winds", *J. Struct. Eng.*, **134**(5), 782-791
Chen, X., Matsumoto, M. and Kareem, A. (2000), "Time domain flutter and buffeting response analysis of bridges", *J. Eng. Mech.- ASCE*, **126**(1), 7-16.
Choi, E.C.C. (2004), "Field measurement and experimental study of wind speed profile during thunderstorms", *J. Wind. Eng. Ind. Aerod.*, **92**, 275-290.
Conte, J.P. and Peng, B.F. (1997), "Fully nonstationary analytical earthquake ground-motion model", *J. Eng. Mech.- ASCE*, **123**(1), 15-24.
Daubechies, I. (1992), *Ten lectures on wavelets*, Society for Industrial and Applied Mathematics, Philadelphia, PA.
Davenport, A.G. (1964), "Note on the distribution of the largest value of a random function with application to gust loading", *P. I. Civil Eng.*, **28**, 187-196.
Deodatis, G. (1996a), "Simulation of ergodic multivariate stochastic processes", *J. Eng. Mech.- ASCE*, **122**(8), 778-787.
Deodatis G. (1996b), "Non-stationary stochastic vector processes: seismic ground motion applications", *Probabilist. Eng. Mech.*, **11**, 149-168.
Fujita, T.T. (1985), *Report of Projects NIMROD and JAWS*, University of Chicago.
Fujita, T.T. (1990), "Downbursts: meteorological features and wind field characteristics", *J. Wind. Eng. Ind. Aerod.*, **36**, 75-86.
Gast, K.D. and Schroeder, J.L. (2003), "Supercell rear-flank downdraft as sampled in the 2002 thunderstorm outflow experiment", *Proceedings of the 11th Int. Conf. on Wind Eng.*, Lubbock ,TX.
Holmes, J.D. (1999), "Modeling of extreme thunderstorm winds for wind loading of structures and risk assessment", *Wind engineering into the 21st century*, *Proceedings of the 10th Int. Conf. on Wind Eng.*, (Eds., Copenhagen, A. Larsen, G.L. Larose, and F.M. Livesey), Balkema, Rotterdam, The Netherlands.
Holmes, J.D. (2007), *Wind loading of structures*, 2nd Ed, Taylor and Francis, London.
Holmes, J.D, Forristall, G. and McConochie, J. (2005), "Dynamic response of structures to thunderstorm winds", *Proceedings of the 10th Americas Conf. on Wind Eng. (10ACWE)* (CD-ROM), Baton Rouge, La..

Holmes, J.D. and Oliver, S.E. (2000), "An empirical model of a downburst", *Eng. Struct.*, **22**, 1167-1172.

Huang, G. and Chen, X. (2009), "Wavelets-based estimation of multivariate evolutionary spectra and its application to nonstationary downburst winds", *Eng. Struct.*, **31**(4), 976-989.

Kim J. and Hangan H. (2007), "Numerical simulations of impinging jets with application to downbursts", *J. Wind. Eng. Ind. Aerod.*, **95**(4), 279-298.

Kwon, D. and Kareem, A. (2009), "Gust-front factor: new framework for wind load effects on structures", *J. Eng. Struct.*, **135**(6), 717-732.

Letchford, C.W. and Chay, M.T. (2002), "Pressure distributions on a cube in a simulated thunderstorm downburst, Part B: moving downburst observations", *J. Wind Eng. Ind. Aerod.*, **90**, 733-753.

Letchford, C.W., Mans, C. and Chay, M.T. (2001), "Thunderstorms-their importance in wind engineering , a case for the next generation wind tunnel", *J. Wind Eng. Ind. Aerod.*, **89**, 31-43.

Li, C., Li, Q., Xiao, Y. and Ou, J. (2012), "A revised empirical model and CFD simulations for 3D axisymmetric steady-state flows of downbursts and impinging jets", *J. Wind Eng. Ind. Aerod.*, **102**, 48-60.

Lutes, L. D. and Sarkani, S. (2004), *Random vibration: analysis of structural and mechanical systems*. Elsevier, NY.

Mason, M. S., Wood, G.S. and Fletcher, D.F. (2009), "Numerical simulation of downburst winds", *J. Wind Eng. Ind. Aerod.*, **97**(11-12), 523-539.

Oseguera, R.M. and Bowles, R.L. (1998), *A simple analytic 3-dimentional downburst model based on boundary layer stagnation flow*, NASA Technical Memorandum No. 100632.

Priestley, M.B. (1981), *Spectral analysis and time series*, Academic, NY.

Sengupta, A. and Sarkar, P.P. (2008), "Experimental measurement and numerical simulation of an impinging jet with application to thunderstorm microburst winds", *J. Wind Eng. Ind. Aerod.*, **96**(3), 345-365.

Solomos, G.P. and Spanos, P.D. (1984), "Oscillator response to nonstationary excitation", *J. Appl. Mech.*, **51**(4), 907-912.

Spanos, P.D. and Failla, G. (2004), "Evolutionary spectra estimation using wavelets", *J. Eng. Mech.- ASCE*, **130**(8), 952-960.

Twisdale, L.A. and Vickery, P.J. (1992), "Research on thunderstorm wind design parameters", *J. Wind Eng. Ind. Aerod.*, **41**(1-3), 545-556.

Wood, G.S., Kwok, K.C.S., Motteram, N.A. and Fletcher, D.F. (2001), "Physical and numerical modeling of thunderstorm downbursts", *J. Wind Eng. Ind. Aerod.*, **89**(6), 535-552.

Vicroy, D.D. (1992), "Assessment of microburst models for downdraft estimation", *J. Aircraft*, **29**(6), 1043-1048.

Xu, Y.L. and Chen, J. (2004), "Characterizing nonstationary wind speed using empirical decomposition", *J. Struct. Eng.- ASCE*, **130**(6), 912-920.

JH